Computational Modeling of Nitric Oxide Formation in Biomass Combustion

Torleif Weydahl, Mette Bugge, Inge R. Gran, and Ivar S. Ertesvåg(*)

Department of Applied Mechanics, Thermodynamics, and Fluid Dynamics
Norwegian University of Science and Technology, N-7491 Trondheim

Department of Thermal Energy, SINTEF Energy Research, N-7465 Trondheim

(*)Author for correspondence: ivar.s.ertesvag@mtf.ntnu.no

Abstract – *Nitric-oxide formation from fuel-bound nitrogen in turbulent non-premixed flames is investigated. The calculations are performed using the k-ε-model for turbulence and the Eddy Dissipation Concept for turbulent combustion in conjunction with detailed chemistry from GRI-Mech 2.11. Comparison with previously measured data shows that the radial profiles for nitric oxide are spread inaccurately, but yields negligible discrepancies for integrated values. Furthermore, to illustrate the potential of the model, preliminary simulations of a wood stove have been performed.*

Introduction

Emission of nitric oxides (NO_x) from combustion processes is a serious threat to our environment. NO_x is the main source of acid rain, ground-level ozone, and photochemical smog. NO_x can be formed by heating air to a high temperature. This is usually the main source of NO_x when oil or natural gas is burned, due to very high peak temperatures. Although peak temperatures typically are low in biomass and coal combustion, NO_x emissions from burning of these fuels are very high since nitrogen is bound to the fuel.

From a computational point of view, biomass combustion presents challenges such as pyrolysis and gasification of solid material, heterogeneous and homogeneous chemical reactions, radiation heat exchange, interaction between solid material and the turbulent reacting flow, interaction between turbulence and combustion, between heat exchange and gasification rate, etc.

By gasification, fuel-bound nitrogen is mainly released in the form of hydrogen cyanide (HCN) and ammonia (NH_3). If these components take part in combustion with excess air, the main part is transformed to nitric oxides.

This paper describes an ongoing work to develop a mathematical model for quantitative prediction of NO_x from nitrogen-containing fuels. Here, the focus is on the gas-phase reactions. The mathematical model is implemented in a CFD code capable of predicting flow and combustion processes in actual combustion equipment. This CFD tool will be used to develop improved combustion devices, such as low-NO_x wood stoves.

In the next section, the mathematical model is described. Then, in the third section, the model is compared with detailed measurements for a jet flame with carefully prescribed boundary conditions. In the section following that, simulation results from an actual wood stove are presented to illustrate the practical potential of the approach. Conclusions and recommendations for further work are given in the final section.

Method and models

The turbulent reacting flow was modeled by the mass-weighted Reynolds-averaged conservation equations for momentum components (the summation convention applies to the spatial indices),

$$\frac{\partial}{\partial t}(\bar{\rho}\tilde{u}_i) + \frac{\partial}{\partial x_j}(\bar{\rho}\tilde{u}_i\tilde{u}_j) = -\frac{\partial \overline{p}}{\partial x_i} + \frac{\partial}{\partial x_j}\left(\overline{\tau}_{ij} - \overline{\rho u_i'' u_j''}\right), \tag{1}$$

energy,

$$\frac{\partial}{\partial t}(\bar{\rho}\tilde{h}) + \frac{\partial}{\partial x_j}(\bar{\rho}\tilde{h}\tilde{u}_j) = \frac{\partial}{\partial x_j}\left(\bar{\rho}\alpha\frac{\partial \tilde{h}}{\partial x_j} - \overline{\rho u_j'' h''}\right) + \overline{S_h}, \tag{2}$$

and mass of all involved species k,

$$\frac{\partial}{\partial t}(\bar{\rho}\tilde{Y}_k) + \frac{\partial}{\partial x_j}(\bar{\rho}\tilde{Y}_k\tilde{u}_j) = \frac{\partial}{\partial x_j}\left(\bar{\rho}\mathcal{D}\frac{\partial \tilde{Y}_k}{\partial x_j} - \overline{\rho u_j'' Y_k''}\right) + \overline{R_k}. \tag{3}$$

The mass-weighted Reynolds-averaged (or Favre-averaged) quantities are defined by $\tilde{\phi} = \overline{\rho\phi}/\overline{\rho}$, where the overbar denotes average (statistical expectation). Although the flow can be regarded "incompressible", that is, with respect to the pressure-density interaction, large density variations will be present in the flame due to variations in composition and temperature.

The turbulence transport was modeled by a turbulence-viscosity model,

$$-\overline{\rho u_i' u_j'} = -\bar{\rho}\widetilde{u_i' u_j'} = \mu_t\left(\frac{\partial \tilde{u}_i}{\partial x_j} + \frac{\partial \tilde{u}_j}{\partial x_i}\right) - \frac{2}{3}\left(\bar{\rho}\tilde{k} + \mu_t\frac{\partial \tilde{u}_l}{\partial x_l}\right)\delta_{ij}, \tag{4}$$

where the turbulence viscosity μ_t was found from the k-ε model (Launder and Spalding, 1974). For turbulent diffusion of energy and mass, the general gradient model was used with a turbulence diffusivity modeled by a constant turbulence Prandtl or Schmidt number.

For flows with a low Mach number, the source term in the energy equation only includes a radiation term. Chemical energy is included in the enthalpy of the individual species.

The Eddy Dissipation Concept for turbulent combustion (EDC) (Magnussen, 1989; Ertesvåg, 2000) was used to model the interaction between turbulence and combustion. When a fast-chemistry assumption (*i.e.* "mixed is burnt") is applied, the average reaction rate is modeled

$$\overline{R}_{\mathrm{fu}} = -\frac{\bar{\rho}\gamma^*\dot{m}^*\chi}{1-\gamma^*\chi}\tilde{Y}_{\mathrm{min}}, \qquad \text{where} \quad \tilde{Y}_{\mathrm{min}} = \min\left(\tilde{Y}_{\mathrm{fu}}, \frac{1}{r}\tilde{Y}_{\mathrm{ox}}\right). \tag{5}$$

Here, r is the stoichiometric oxidizer (air) requirement for the specific fuel, and subscripts fu and ox denote fuel and oxidizer, respectively. The quantities γ^* and $\dot{m}^*$ are the mass

fraction of turbulence fine structures and its mass exchange with the surrounding fluid, respectively. These are related to the turbulence-cascade model of the EDC (see Ertesvåg and Magnussen, 2000; Ertesvåg, 2000) and are expressed as functions of the turbulence energy k and turbulence-energy dissipation rate ε. The chemical reactions are assumed to occur in the fine structures, i.e., the smalle turbulence scales. The mass exchange is the reciprocal of the fine-structure residence time, $\tau^* = 1/\dot{m}^*$, which is proportional to the Kolmogorov time scale. The quantity χ is the fraction of fine structure that is reacting, and is a function of the concentrations of fuel, oxidizer and product.

The implementation of chemical kinetics is described by Gran and Magnussen (1996). Then the reaction rate for a chemical species is expressed

$$\overline{R}_k = -\frac{\bar{\rho}\gamma^*\dot{m}^*}{(\gamma^*)^{1/3}}(Y_k^o - Y_k^*). \tag{6}$$

Here Y_k^o and Y_k^* is the mass fraction into and out of the fine-structure reactor. The reacting turbulence fine structure is regarded as a perfectly stirred reactor, and the mass balance in the reactor is expressed

$$\frac{dY_k}{dt} = \omega_k^* + \nu_r(Y_k^o - Y_k^*) \tag{7}$$

for each species k. Here, the reactor mixing rate is $\nu_r = 1/\tau^*$, and $\omega_k^* = R_k^*/\rho^*$ is the specific reaction rate found from chemical-kinetics data from GRI-Mech 2.11 (Bowman *et al.*) These species mass balances, together with balances for energy and momentum, are solved for the reactor by integrating to steady state.

Ammonia doped jet flame

In this section, the ability of the Eddy Dissipation Concept (EDC) for turbulent combustion with detailed chemistry to predict the conversion of ammonia to nitric oxides is assessed. The best way of achieving this is to compare the model with data from detailed measurements of well-defined laboratory flames.

Experimental data for comparison

The present simulations were compared with measurements performed by Lapp et al. (1983) and later reported by Drake *et al.* (1984). The horizontal fuel jet, which emerged from a 3.2 mm diameter nozzle with an average flow of 54.6 m/s, was centered in a channel air flow of 2.4 m/s. The molar composition of the fuel was 39.7%, 29.9%, 29.7% and 0.7% for CO, H_2, N_2, and CH_4, respectively. CH_4 was removed from the gas mixture when thermal NO was investigated. Ammonia was added in amounts varying from 0.0% to 1.64%. Laser velocimetry and pulsed Raman scattering provides data for mean and rms of velocity, temperature, and major species concentrations. Formation of nitric oxide was experimentally analyzed by probe sampling 100 diameters downstream of the nozzle outlet.

Modeling approach

The present predictions were made using the general-purpose CFD code Spider, which is based on finite volumes and non-orthogonal curvilinear computational mesh. In this case,

a 2-dimensional rectangular mesh with axial symmetry was used. Hence, the buoyancy of the horizontal flame was neglected. Radiation was not taken into account in the calculations presented here, resulting in a generally over-predicted temperature.

The jet flame was first predicted with the fast-chemistry assumption, that is, with the reaction rate from Eq. 5. The calculations were made with a 50×28 control-volume grid, where the upstream boundary coincided with the nozzle outlet. The jet inlet boundary conditions were taken from simulations of a separate pipe simulation corresponding to the fuel-jet tube flow. This case was also simulated with a 68×28 control-volume grid. Then, a 90 mm long fuel-jet tube, and the flows inside and outside this tube, were included in the simulations by blocking out a volume corresponding to the tube material. The results from these two approaches were very close to each other (Weydahl, 2000).

Turbulence was modeled by the k-ε model using standard constants $C_{\varepsilon 1}$ and $C_{\varepsilon 2}$ equal to 1.44 and 1.92, respectively. It was also simulated with values 1.44 and 1.79, 1.44 and 1.83, and with 1.60 and 1.92. From this and other simulations, it seems that the combination of $C_{\varepsilon 1} = 1.44$ and $C_{\varepsilon 2} = 1.83$, together with turbulence Prandtl and Schmidt numbers of $\sigma_h = \sigma_Y = 0.5$, gives the best representation of the reacting turbulent round-jet flow.

In the detailed-chemistry approach, the transport and reactor balance equations (Eqs. 3 and 6) were solved for 49 chemical species taking part in 277 elementary reactions. These calculations were made with the 50×28 control-volume grid, starting at the nozzle outlet with inlet boundary conditions taken from a separate fuel-jet tube pipe simulation (see above).

Results and discussion

Predicted results for axial velocity were generally in satisfactory agreement with measurements. It is known that the standard k-ε turbulence model over-predict the spreading of a round jet. The modification mentioned above gave the best approach to the dataset. Nevertheless, the mixture-fraction profile through the flame were in varying agreement. (Mixture fraction is defined, e.g., in Ertesvåg (2000) p. 84.) The profile at $x/d = 50$ in Fig. 1 shows only negligible discrepancies with the experiments, whereas calculated values at $x/d = 10$ are more spread. Here, d is the internal diameter of the nozzle and x is the axial distance from the nozzle outlet.

The NO values were measured at $x/d = 100$. In Fig. 2(b), measurements and predictions of NO are compared for 0.8% ammonia added. The calculated profile is less spread than the experimental profile. This corresponds with the temperature profile in Fig. 2(a). The general discrepancy in spreading at this position in the flame also leads to the over-predicted peak values seen in Fig. 3(a). However, the integrated values shown in Fig. 3(b) are, may be by some fortune, in good agreement with measured values and yields better accuracy than previous predictions.

The previous predictions for NO_x in Fig. 3(b) are reproduced from Drake *et al.* (1984) who used a k-ε-model, combined with an assumed probability- density function for species from conservation of the mixture fraction, and a simplified mechanism for thermal and fuel NO. For thermal NO_x, the integrated value was measured to $5.26 \cdot 10^{-8}$ kg/s, whereas present calculation gave $13.0 \cdot 10^{-8}$ kg/s. This is mainly due to the higher peak temperatures in the calculations compared with the measurements. The predictions by Drake *et al.* (1984), on the other hand, under-predicted thermal NO_x ($1.7 \cdot 10^{-8}$ kg/s), although the temperature

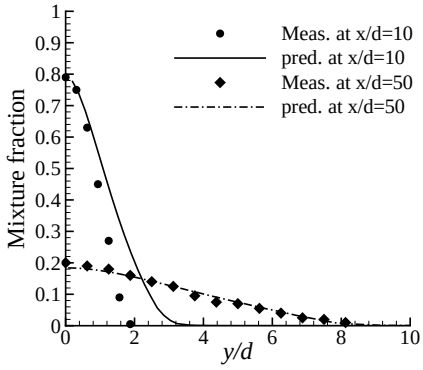

Figure 1: Comparison of measurements and predictions of mixture fraction at $x/d = 10$ and $x/d = 50$.

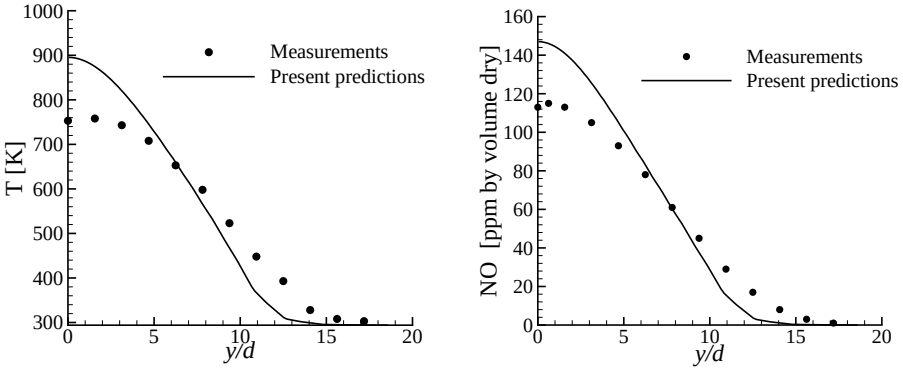

(a) Temperature profile at x/d=100

(b) NO profile at x/d=100. 0.8% NH_3 is added

Figure 2: Comparison of measurements and predictions of temperature and NO.

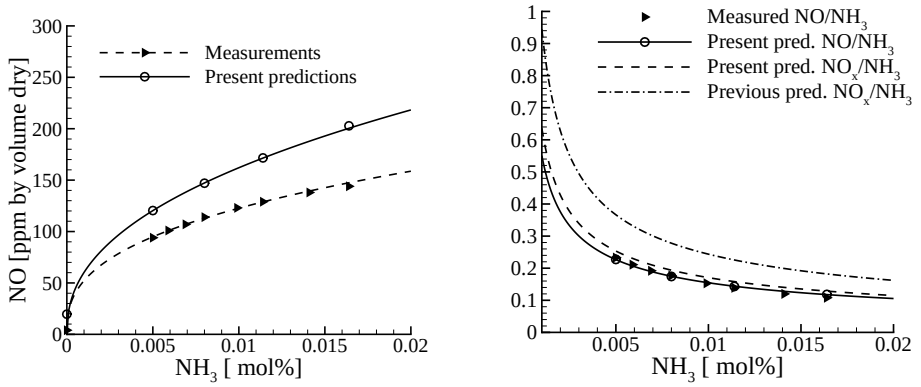

(a) Peak values at x/d=100 for various added NH_3

(b) Radially integrated values at x/d=100

Figure 3: Comparison of measurements and present and previous predictions for the molar yield of NO and NO_x from NH_3.

from these predictions also was higher.

The results shown in Figs. 4(b) and 5 point towards a possible approach in studying the conversion rate of ammonia in turbulent combustion. The graphs represent the radially integrated production or reduction rate of NO for a particular chemical reaction. Based on theory for NH_3 oxidation (Miller and Bowman, 1989), some reactions important for NO formation and reduction included in the GRI-Mech 2.11 are investigated. Figure 4(a) gives a view of how the species in these reactions are acting to form and reduce NO. In Fig. 4(b), the radially integrated production rate of thermal NO is plotted as a function of the axial position in the flame. The figure shows where the three reactions of the Zeldovich mechanism are of greatest importance.

Similarly, the rate of production and reduction of NO by these and other selected chemical reactions are plotted in Fig. 5 for 0.8% NH_3 added. The first reaction in the Zeldovich mechanism is consuming NO upstream of $x/d = 32$ (Fig. a) and producing NO further downstream (Fig. c). Likewise, the radical NH acts both as a producing and reducing agent for NO (Figs. b and d).

Integrated values for NO formed from fuel-bound nitrogen are generally in good agreement with experimental data. However, some discrepancies in the distribution of NO are observed. Figure 2 shows that the spreading of the temperature (i.e. energy) and chemical species is underpredicted, leading to too high peak values. Further upstream, the temperature field of the major part of the flame is overpredicted. (The uncertainty of the experimental data is estimated to at least ± 50 K by the datatakers (Drake *et al.*, 1984). This indicates that the reactions occur somewhat close to the nozzle. And this, in turn, may be attributed to the higher temperature; that is, a self-enhancing process. Some of the discrep-

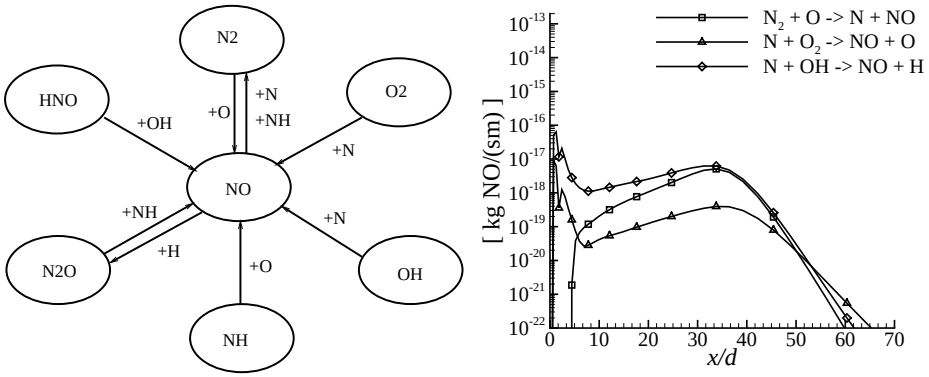

(a) Scheme for reactions selected for plotting

(b) Rate of NO produced by Zeldovich mechanism

Figure 4: (a) An overview of selected reacting species in NO formation with ammonia addition. (b) Rate of NO produced by the Zeldovich mechanism with no NH_3 or CH_4 added.

ancy, in particular far downstream, can be explained by the deviation from axisymmetry of the horizontal experimental flame due to buoyancy.

Two important reasons for the discrepancies of the temperature predictions are the lack of radiation model and the insufficient representation of the reacting jet flow by the k-ε-model. Actually, the standard version of the turbulence model gives a lower peak temperature, and therefore less thermal NO production. Then, however, the velocity field is poorly predicted. Since the round jet also is a considerable challenge also for newer, more advanced and complex turbulence models, the solution may be an especially designed *ad-hoc* jet-flame turbulence model for combustion model development.

Further work is being carried out on implementing a radiation model. As this flame can be approximated as an optically thin flame, a simple radiant emission model can be applied for the major species. Preliminary results indicate a general temperature reduction of about 50 to 100 K. They also indicate that H_2 reactions are moved towards the nozzle and CO reactions are moved downstream.

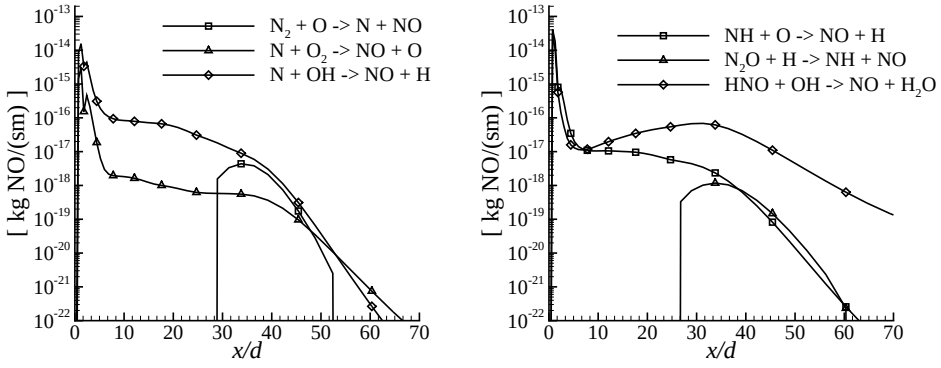

(a) NO production rate **(b)** NO production rate

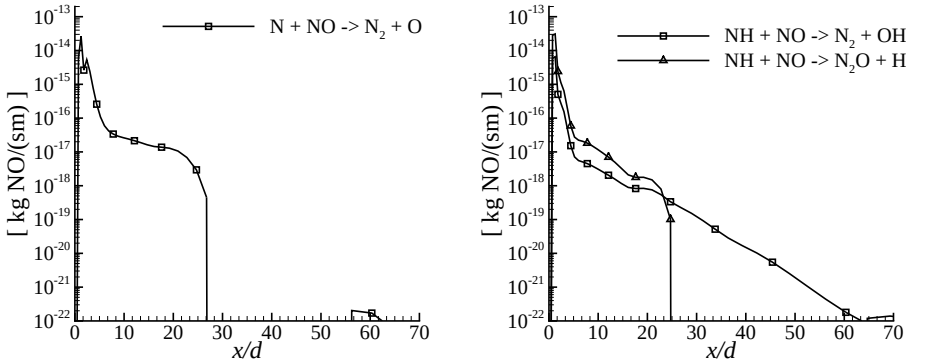

(c) NO reduction rate **(d)** NO reduction rate

Figure 5: Rate of NO produced and reduced from NH_3, radially integrated. NH acts both as a producing and reducing agent for NO.

Wood log combustion

The previous section shows that the CFD model is capable of predicting NO_x levels in carefully controlled laboratory flames with ammonia addition. To illustrate the potential of the model, preliminary simulations of a realistic wood stove have been performed.

Design of the wood stove

A typical design of the wood stove was selected, Fig. 6. The horizontal plate runs across the stove (normal to the plane of the paper), and the width of the stove in this direction is 300 mm. The combustion air is injected stepwise. Primary air is injected in the first reaction zone. The wood fuel is gasified and the gases released from the wood logs start to combust. Preheated secondary air is injected to ensure complete burnout.

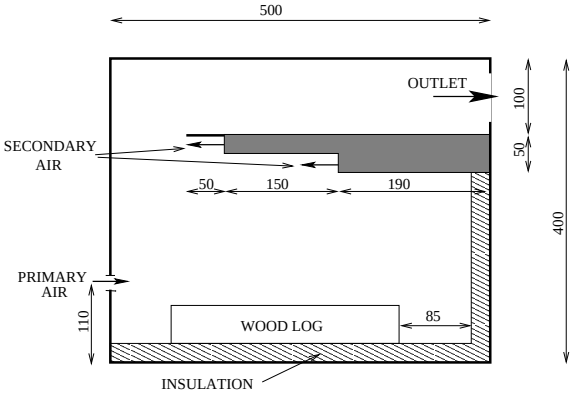

Figure 6: Wood stove design (dimensions in mm; the width normal to the plane is 300 mm).

Modeling approach

A Cartesian grid with $45 \times 17 \times 45 = 34425$ grid nodes was used to model the geometry of the wood stove in the CFD-code KAMELEON FireEx. A symmetry boundary was chosen at the center plane parallel to the paper plane of Fig. 6.

The following data used are typical data for realistic wood stoves. The heat transfer through all the outer walls was calculated with a constant surface temperature at the outer surface of the wall as boundary condition. The cast-iron walls all around the stove were 0.5 cm thick. The bottom, back and sidewalls of the stove had 2.5 cm insulation inside the cast-iron wall. The specified surface temperature at these walls is 353 K. At the front and on the top, the surface temperature was 573 K and 473 K, respectively. The thermal properties for the insulation and the cast iron are shown in Table 1.

Three wood logs with dimensions 0.3 m $\times$ 0.05 m $\times$ 0.05 m were placed in the stove. Gaseous fuel was released from the top of the wood logs at a low velocity (0.011 m/s). The flow rate was 1.57 kg/h and the temperature 341.4 K. The molar composition of the gas is shown in Table 2.

Table 1: Thermal properties used for cast-iron and insulation.

Material	Thermal conductivity [W/mK]	Density [kg/m^3]	Heat capacity [J/kgK]	Emissivity
Cast-iron	60	7190	460	0.95
Insulation	0.3	950	700	0.81

Table 2: Molar composition [%] of the released gas.

CH_4	CO_2	CO	H_2O	N_2	NO	NH_3
33.93598	25.88643	9.30966	30.77901	0.02964	0.02964	0.02964

The primary air was released horizontally through an inlet in the front wall located at the center of the wall just above the wood logs. The secondary air was injected horizontally through nozzles at two locations at the underside of the horizontally plate that runs across the stove. The nozzles were spread over the width of the plate. The secondary air was preheated to 473 K and 523 K, respectively, before it was released at the two different locations. The primary reaction zone had 70% stoichiometric air (*i.e.* $\lambda = 0.70$, $\phi = 1/0.70 = 1.43$), whereas the overall stoichiometric air was 150% ($\lambda = 1.5$; *i.e.* fuel lean).

The horizontal plate influences the flow field in the stove significantly and forces the combustion gases to flow around the plate instead of straight to the outlet.

The combustion of methane and CO was modeled with a single-step mechanism according to Eq. 5. The discrete transfer model by Lockwood and Shah (1981) was used to model radiation. This model includes radiative heat exchange from participating gases and surrounding solid surfaces.

Results and discussion

Temperature, velocity field and mass fraction of O_2 and CH_4 are shown in the same vertical plane along the stove near the centerline, Figs. 7(b), 8(a), and 8(b). The highest temperatures are in the primary area above the wood log and here all the oxygen is consumed. The maximum temperature (1370 K) was relatively low. This was due to the low calorific value of the fuel gas, to the under-stoichiometric combustion in the primary zone, and to the radiative heat transfer to the walls. The excess of fuel burns out as the secondary air is injected.

Figure 7(a) shows the temperature in a vertical plane across the stove at $x = 0.106\,\mathrm{m}$. The primary air is supplied through an opening at the center of the front wall. In the figure, a colder zone due to the primary air inlet can be recognized above the wood log in center. This colder zone, and also the secondary-air zone, can also be recognized in Fig. 7(b) and especially in Fig. 8(a).

Maximum values of the temperature are projected into a vertical plane along the stove in Fig. 9. This field represents what temperatures that the side walls see. Maximum calculated gas temperature is 1371 K.

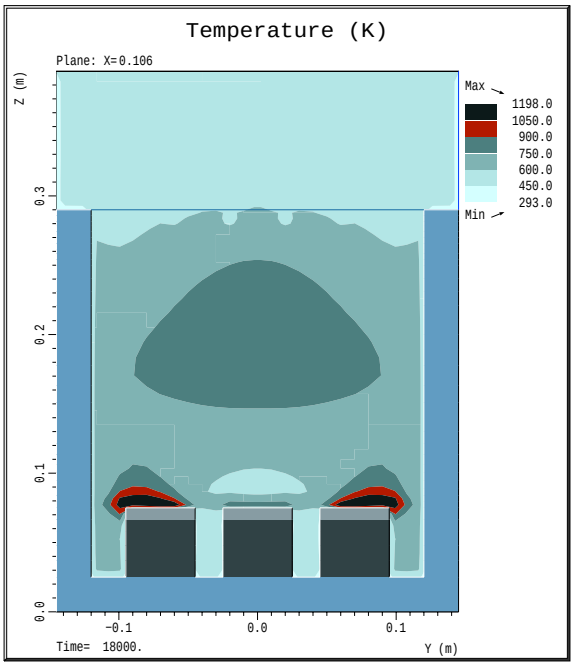

(a) Across the wood stove

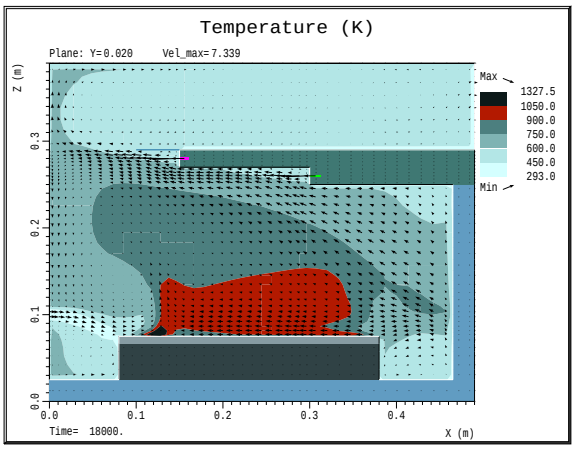

(b) Along the wood stove

Figure 7: Temperature [K] in two different vertical planes.

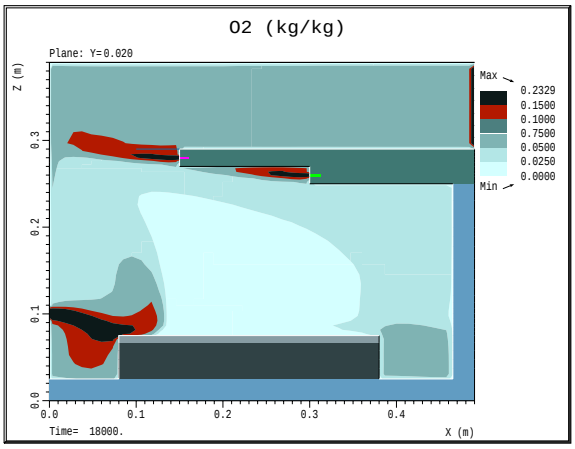

(a) Mass fraction of O_2

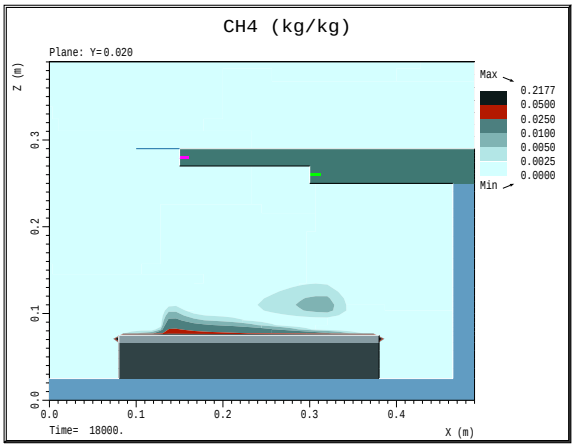

(b) Mass fraction of CH_4

Figure 8: Mass fractions [kg/kg] in a vertical plane along the wood stove.

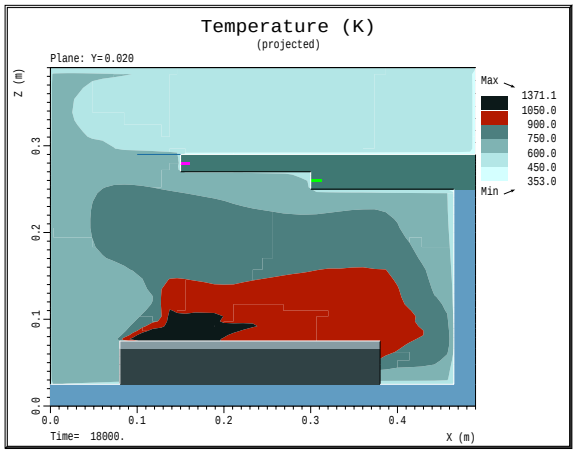

Figure 9: Maximum temperatures [K] projected into a vertical plane along the stove.

The predicted mean temperature at the outlet was 520 K. This is in satisfactory agreement with the expected temperature level.

Production of thermal NO_x is insignificant at temperatures below 1700 K. According to this and the fact that wood contains nitrogen, it is necessary to include detailed mechanisms for the chemistry in the calculations to be able to study NO_x reduction in wood-stove combustion. This will be our next step in this work.

Concluding remarks

Nitric oxides (NO_x) is one of the main pollutants resulting from combustion processes. NO_x emissions are particularly high from fuels containing nitrogen, such as biomass and coal. Mathematical models describing NO_x formation can contribute to the reduction of NO_x emissions by assisting the improved design and operation of combustion equipment.

A mathematical model for turbulent combustion featuring a detailed description of elementary chemical reactions has been implemented in the in-house CFD code Spider. Comparison with experimental results shows that the overall effects of NO_x formation from fuel-bound nitrogen are captured by the model.

Three-dimensional simulations of flow, combustion, and radiation inside an actual wood stove illustrate the practical potential of the approach. Further work includes performing simulations of the wood stove using the same detailed chemistry scheme as for the jet flame.

Acknowledgments

We are grateful to a colleague, Dr. Øyvind Skreiberg, for providing the data on the wood stove and released gas, and for useful discussions with him.

References

Bowman, C.T, R.K. Hanson, D.F. Davidson, W.C. Gardiner Jr., V. Lissianski, G.P. Smith, D.M. Golden, M. Frenklach, M. Goldenberg *Gri-Mech 2.11*
`http://www.me.berkeley.edu/gri_mech/`

Drake, M.C., R.W. Pitz, S.M. Correa, M. Lapp 1984 Nitric oxide formation from thermal and fuel-bound nitrogen sources in a turbulent nonpremixed syngas flame. *20th Symp. (Int.) Comb.:* 1983-1990

Ertesvåg, Ivar S. 2000 *Turbulent strøyming og forbrenning.* ("Turbulent flow and combustion"; in Norwegian.) Tapir Academic Publisher, Trondheim.

Ertesvåg, Ivar S., Bjørn F. Magnussen 2000 The Eddy Dissipation turbulence energy cascade model. *Comb. Sci. Technol. 159:* 213-236.

Gran, Inge R., Bjørn F. Magnussen 1996 A numerical study of a bluff-body stabilized diffusion flame. Part 2. Influence of combustion modeling and finite-rate chemistry. *Comb. Sci. Technol. 119:* 191-217.

Lapp, M., M.C. Drake, C.M. Penney, R.W. Pitz, S. Correa 1983 *Turbulent combustion experiments and modeling.* Final report prepared for Power Systems Division, U.S. Dept. Energy, Washington D.C.

Launder, B.E., D.B. Spalding 1974 The numerical computation of turbulent flows. *Computer Methods in Appl. Mech. and Eng. 3:* 269-289.

Lockwood, F.C., N.G. Shah 1981 A new radiation method for incorporation in general combustion prediction procedures. *Eighteenth Symp. (Int.) Comb.:* 1405-1413. Comb. Inst., Pittsburgh, Pennsylvania.

Magnussen, Bjørn F. 1989 Modeling of NO_x and soot formation by the Eddy Dissipation Concept. *Int. Flame Research Foundation, 1st Topic Oriented Technical Meeting.* 17-19 Oct., Amsterdam, Holland.

Miller, J.A., C.T. Bowman 1989 Mechanism and modeling of nitrogen chemistry in combustion. *Prog. Energy Combust. Sci. 15:* 287-338.

Weydahl, Torleif *Danning og reduksjon av nitrogenoksid i forbrenning.* ("Formation and reduction of nitric oxides in combustion", in Norwegian.) Diploma work, Department of Applied Mechanics, Thermodynamics, and Fluid Dynamics, Norwegian University of Science and Technology, Trondheim, December 2000.